Direct-drive inertial confinement fusion research at the Laboratory for Laser Energetics: charting the path to thermonuclear ignition

R.L. McCrory[1,2]**, S.P. Regan**[1]**, S.J. Loucks**[1]**, D.D. Meyerhofer**[1,2]**, S. Skupsky**[1]**,**
R. Betti[1,2]**, T.R. Boehly**[1]**, R.S. Craxton**[1]**, T.J.B. Collins**[1]**, J.A. Delettrez**[1]**, D. Edgell**[1]**,**
R. Epstein[1]**, K.A. Fletcher**[3]**, C. Freeman**[3]**, J.A. Frenje**[4]**, V.Yu. Glebov**[1]**,**
V.N. Goncharov[1,2]**, D.R. Harding**[1]**, I.V. Igumenshchev**[1]**, R.L. Keck**[1]**,**
J.D. Kilkenny[1,5]**, J.P. Knauer**[1]**, C.K. Li**[4]**, J. Marciante**[1]**, J.A. Marozas**[1]**,**
F.J. Marshall[1]**, A.V. Maximov**[1]**, P.W. McKenty**[1]**, J. Myatt**[1]**, S. Padalino**[3]**,**
R.D. Petrasso[4]**, P.B. Radha**[1]**, T.C. Sangster**[1]**, F.H. Séguin**[4]**, W. Seka**[1]**,**
V.A. Smalyuk[1]**, J.M. Soures**[1]**, C. Stoeckl**[1]**, B. Yaakobi**[1] **and J.D. Zuegel**[1]

[1] Laboratory for Laser Energetics, University of Rochester, Rochester, NY, USA
[2] Departments of Mechanical Engineering and Physics and Astronomy, University of Rochester, Rochester, NY, USA
[3] SUNY Geneseo, Geneseo, NY, USA
[4] Plasma Science and Fusion Center, MIT, Cambridge, MA, USA
[5] General Atomics, San Diego, CA, USA

E-mail: rmcc@lle.rochester.edu

Abstract
Significant theoretical and experimental progress continues to be made at the University of Rochester's Laboratory for Laser Energetics (LLE), charting the path to direct-drive inertial confinement fusion (ICF) ignition. Direct drive offers the potential for higher-gain implosions than x-ray drive and is a leading candidate for an inertial fusion energy power plant. LLE's direct-drive ICF ignition target designs for the National Ignition Facility (NIF) are based on hot-spot ignition. A cryogenic target with a spherical DT-ice layer, within or without a foam matrix, enclosed by a thin plastic shell, will be directly irradiated with ~1.5 MJ of laser energy. Cryogenic and plastic/foam (surrogate-cryogenic) targets that are hydrodynamically scaled from these ignition target designs are imploded on the 60-beam, 30 kJ, UV OMEGA laser system to validate the key target physics issues, including energy coupling, hydrodynamic instabilities and implosion symmetry. Prospects for direct-drive ignition on the NIF are extremely favourable, even while it is in its x-ray-drive irradiation configuration, with the development of the polar-direct-drive concept. A high-energy petawatt capability is being constructed at LLE next to the existing 60-beam OMEGA compression facility. This OMEGA EP (extended performance) laser will add two short-pulse, 2.6 kJ beams to the OMEGA laser system to backlight direct-drive ICF implosions and study fast-ignition physics with focused intensities up to 6×10^{20} W cm^{-2}.

PACS numbers: 52.57.-z, 52.57.Bc, 52.57.Fg, 52.57.Kk

(Some figures in this article are in colour only in the electronic version)

1. Introduction

Direct-drive inertial confinement fusion (ICF) offers the potential for higher-gain implosions than x-ray drive and is a leading candidate for an inertial fusion energy power plant [1]. The achievement of thermonuclear ignition and high gain in the laboratory with direct-drive ICF requires a physical understanding of the entire implosion process. Significant theoretical and experimental progress in charting this path to ignition continues to be made at the University of Rochester's Laboratory for Laser Energetics (LLE). Direct-drive ICF is also actively studied at the Naval Research

Laboratory (USA) [2] and the Institute for Laser Engineering (Japan) [3].

LLE's direct-drive ICF ignition target designs for the National Ignition Facility (NIF), or other MJ-class lasers, rely on hot-spot ignition [4], where a cryogenic target with a spherical DT-ice layer, within or without a foam matrix, enclosed by a thin plastic shell will be directly irradiated with ~1.5 MJ of laser energy [5]. During an implosion, the main fuel (DT-ice) layer will compress the residual DT gas, forming a central hot spot. A thermonuclear burn wave is predicted to propagate through the main fuel layer when the hot spot's fuel areal density reaches ~0.3 g cm^{-2} with a temperature of ~10 keV [4]. Our research shows that high-gain (~35) ignition with the baseline direct-drive target design is likely on the NIF [5, 6]. The NIF, under construction at the Lawrence Livermore National Laboratory, is a 1.8 MJ, 351 nm, 192-beam laser system [7].

The path to ignition is being explored with hydrodynamically scaled, direct-drive-implosion experiments on the 60-beam, 30 kJ OMEGA laser system [8]. These experiments are validating the hydrodynamic codes used to design high-gain, cryogenic-DT ignition targets. Targets are imploded to investigate the key target physics issues of energy coupling, hydrodynamic instabilities and implosion symmetry. The performance of imploding cryogenic-D_2 capsules on OMEGA [6, 9] is close to the predictions of the two-dimensional hydrodynamic code *DRACO* [10]. This research gives high confidence that direct-drive implosions will ignite on the NIF with symmetric illumination.

The NIF will be initially configured for x-ray drive, with no equatorial beams to symmetrically irradiate a direct-drive target. Although the implementation of the direct-drive beam configuration is not currently scheduled until 2014, prospects for direct-drive ignition on the NIF while it is in its x-ray-drive irradiation configuration are favourable with the development of polar direct drive (PDD) [11]. The PDD approach is based on the optimization of phase-plate design, beam pointing and pulse shaping to provide uniform drive with nonsymmetric beam locations. Initial two-dimensional simulations of the PDD target design have shown ignition with modest gain [11]. PDD simulations are being validated by experiments on OMEGA [12].

Fast ignition (FI) [13] is a complementary approach to hot-spot ignition and an active area of research at LLE. In this concept, a target is compressed without the formation of a hot spot. At peak compression a high-energy petawatt (HEPW) laser provides the 'spark' energy to begin the ignition process. An HEPW capability is being constructed at LLE adjacent to the existing OMEGA compression facility. The OMEGA EP (extended performance) laser will add two short-pulse (~10 ps-duration), 2.6 kJ beams to the OMEGA laser system to study FI physics with focused intensities up to 6×10^{20} W cm^{-2} for experiments beginning in 2008. Direct-drive fuel assembly experiments with FI cone targets have begun on OMEGA, and a substantial fraction of the predicted core areal density has been measured [14, 15].

This paper provides an overview of the direct-drive target physics programme at LLE. A general description of direct-drive ICF and the techniques used to mitigate the effects of hydrodynamic instabilities is given in section 2. Symmetric direct-drive implosions of high-performance scaled cryogenic targets on OMEGA and the predicted performance of LLE's baseline direct-drive target design for the NIF are presented in section 3. PDD for the NIF and PDD experiments on OMEGA are discussed in section 4. A brief description of the OMEGA EP is given in section 5, along with the results from FI fuel assembly experiments. The conclusions are presented in section 6.

2. Direct-drive ICF

A direct-drive implosion is initiated by the ablation of material from the outer surface of a spherical shell containing thermonuclear fuel with intense laser beams [4, 5]. The ablated shell mass forms a coronal plasma that surrounds the target and accelerates the shell inwards via the rocket effect [4]. Since ICF target acceleration and subsequent deceleration occur while hot, low-density plasma pushes against (accelerates/decelerates) a cold, high-density plasma, the target implosion is unstable to the Rayleigh–Taylor instability (RTI) [4–6, 16]. The implosion can be divided into four stages: early time, acceleration phase, deceleration phase and peak compression. Perturbation seeds early in the implosion from single-beam laser non-uniformities (imprint), laser drive asymmetry and the outer/inner-shell-surface roughnesses determine the final capsule performance. The unstable RTI growth is controlled by reducing the seeds (e.g. laser imprint and target-surface roughness) and the growth rates of the dominant modes. These perturbations feed through the shell during the acceleration phase and seed the RTI of the deceleration phase at the inner shell surface [17]. When the higher-density shell converges towards the target centre and is decelerated by the lower-density hot-spot plasma, the RTI causes mixing of the shell material with the hot spot (i.e. shell mix) [18]. Modulations also grow owing to Bell–Plesset convergent effects throughout the implosion [19, 20]. The thermonuclear fusion rate increases as the compression heats the hot spot and increases its fuel areal density. Predictions show that alpha-particle heating causes a thermonuclear burn wave to propagate through the main fuel layer when the fuel areal density of the central hot spot reaches ~0.3 g cm^{-2} with a temperature of ~10 keV [4]. Ultimately, the RTI deceleration phase can disrupt the central hot-spot formation and prevent it from igniting. An understanding of the RTI-induced mix and developing ways to control it are of great importance to the goal of achieving thermonuclear ignition in the laboratory.

The target physics research programme at LLE combines all aspects of direct-drive ICF including early-time phenomena such as plasma formation and laser-beam imprinting, RTI growth during the acceleration and deceleration phases, shell mix at peak burn and shock timing and coalescence. High-performance cryogenic and mass-equivalent gas-filled-plastic-shell (i.e. warm surrogate) implosions are studied. Surrogate targets are used to develop an understanding of the physics of capsule implosions without being encumbered by the technological complications associated with cryogenic targets. Target performance is diagnosed by neutronics [21], charged-particle spectroscopy [22, 23], x-ray spectroscopy [24] and x-ray imaging [25]. OMEGA creates extreme states of matter
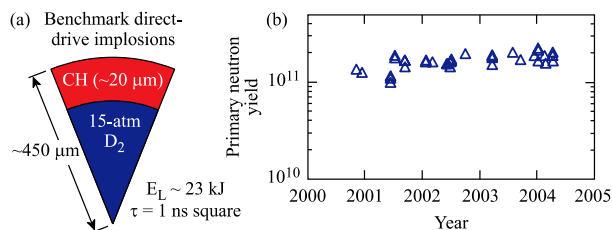
Figure 1. (*a*) Schematic of a benchmark deuterium-filled plastic-shell target having a ∼450 μm radius, a 20 μm shell thickness and a 15 atm D_2 fill pressure. (*b*) The measured primary neutron yield of a benchmark target on OMEGA has been highly reproducible over the last four years.

with high reproducibility. An example of such performance is shown in figure 1, which presents the measured primary neutron yield over the past four years of a benchmark implosion of a 15 atm, deuterium-filled, 20 μm thick plastic-shell target irradiated with a 23 kJ, 1 ns square laser pulse on OMEGA. The measured primary neutron yield has a 16% standard deviation over this period, owing to the excellent control of the on-target laser irradiation and the high quality of the deuterium-filled, plastic-shell targets.

Laser imprint levels are reduced by creating a uniform laser irradiation of the target. High-compression direct-drive experiments require a ∼1% rms level of on-target laser irradiation non-uniformity averaged over a few hundred picoseconds [26]. This is accomplished on the OMEGA laser system using two-dimensional smoothing by spectral dispersion (two-dimensional SSD) [27–29], distributed phase plates (DPPs) [30, 31], polarization smoothing (PS) using birefringent wedges [32–37] and multiple-beam overlap [38]. These techniques have been demonstrated on OMEGA [39][1] and are directly applicable to direct-drive ignition target designs planned for the NIF [5,6]. Induced spatial incoherence is an alternative smoothing technique that is employed on the NIKE laser system [40].

Recently, the laser irradiation non-uniformity was reduced on OMEGA with a new DPP [38, 41]. The envelope of the single-beam, far-field intensity has a super-Gaussian shape, $I(r) \propto \exp[-(r/\delta)^n]$, where r is the radius of the beam, δ is the 1/e half-width and n is the super-Gaussian order. The new SG4 DPP with $n = 4.1$ and $\delta = 357\,\mu$m produces a more azimuthally symmetric far field, and has replaced the SG3 DPP with $n = 2.3$ and $\delta = 308\,\mu$m. The low-ℓ-mode ($3 < \ell < 8$) non-uniformity level was significantly reduced, as were selected modes in the intermediate range ($10 < \ell < 80$) [41]. The effects of the low- and intermediate-ℓ-mode non-uniformities on the target performance of high-adiabat, deuterium-filled-plastic-shell implosions were investigated [41]. Implosions are categorized by the adiabat α or isentrope parameter of the shell, which is defined as the ratio of the shell pressure to the Fermi-degenerate pressure [4]. Target performance is quantified by the ratio of measured primary neutron yield to one-dimensional predicted yield, which is defined as the yield over clean (YOC). Figure 2 shows that the YOC for 3 atm deuterium-filled, high-adiabat ($\alpha \sim 7$), plastic-shell implosions with 27 μm thick

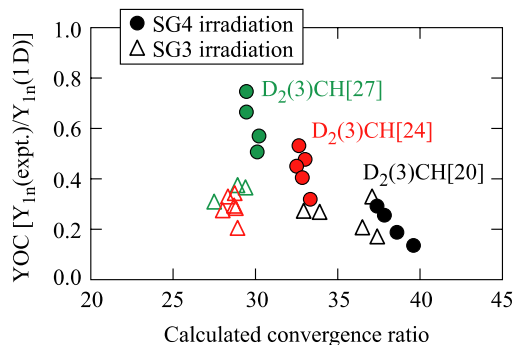[1] Copies may be obtained from the National Technical Information Service, Springfield, VA 22161.

Figure 2. The ratio of measured primary neutron yield to the one-dimensional predicted YOC for 3 atm deuterium-filled, high-adiabat, plastic-shell implosions is plotted as a function of the calculated convergence ratio for the SG3 and SG4 irradiation conditions. The new SG4 DPP with $n = 4.1$ and $\delta = 357\,\mu$m, which produces a more azimuthally symmetric far field, replaced the SG3 DPP with $n = 2.3$ and $\delta = 308\,\mu$m. As a result, the low-ℓ-mode ($3 < \ell < 8$) non-uniformity level was significantly reduced, as well as select modes in the intermediate range ($10 < \ell < 80$).

shells increased by almost a factor of 2 with the reduced non-uniformity, while the YOC for the 20 μm thick shells remained unchanged. The target performance of the more unstable, thinner-shell target is less sensitive to the reduced long-wavelength non-uniformities because it is dominated by the very short-wavelength, single-beam-irradiation non-uniformities [10]. In contrast, the thicker-shell target is less susceptible to the laser imprint from the high-ℓ modes and more sensitive to the reduction in the low- and intermediate-ℓ-mode non-uniformities [10].

The RTI growth rate is approximately $\gamma = \alpha_{RT}\sqrt{kg} - \beta_{RT}kV_a$, where $\alpha_{RT} = 0.94$ and $\beta_{RT} = 2.6$ for a DT ablator, k is the perturbation wave number, g is the acceleration and the ablation velocity V_a is proportional to $\alpha^{3/5}$ [42]. Increasing α at the ablation surface reduces γ; however, α at the inner portion of the shell determines the minimum energy required for ignition, $E_{min} \sim \alpha^{1.88}$ [43,44]. If α is uniform throughout the shell, there is a trade-off between target gain and stability. This trade-off can be avoided by tailoring the adiabat of the shell to optimize γ and E_{min}. Shaping the adiabat α of the shell, with α larger at the ablation surface, increases V_a and reduces γ, while the lower α in the inner portion of the shell (main fuel layer), maintains the compressibility of the target and maximizes the yield [45].

Adiabat shaping is achieved by launching an unsupported shock wave into the shell with a short (∼100 ps), intense Gaussian laser pulse ('picket') at the beginning of the implosion [2, 45]. Alternatively, the adiabat can be shaped by relaxing the shell density with a weak laser prepulse, followed by a power shutoff prior to the foot of the main laser drive pulse [46, 47]. Picket-pulse shapes for direct-drive ignition were first proposed in [48]. The main motivation for such pulses was to replace the continuous shell acceleration with an impulsive acceleration. The impulsive acceleration leads to a linear-in-time growth, replacing the exponential RT growth. Also, in [49] a short picket in front of the main pulse was introduced to dynamically produce a tailored density profile that reduces laser imprinting during the early stage of the implosion. The idea of adiabat shaping has also been designed
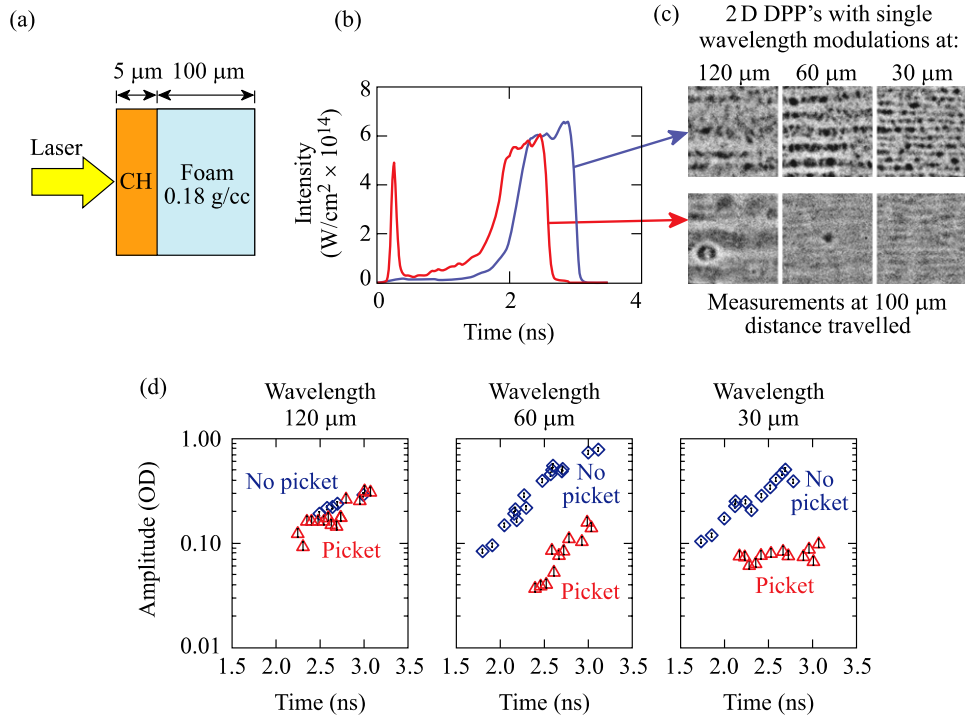
Figure 3. (*a*) Warm surrogate foam target used in planar RTI x-ray radiography experiment to investigate the effects of the picket; (*b*) low-adiabat laser pulse shapes with and without the picket. (*c*) Measured radiographs show significant laser imprint reduction with the picket pulse. (*d*) Optical-depth modulations are significantly reduced at shorter wavelengths using the picket pulse.

for an ignition target using x-ray preheat, which is different from the concept presented here [16].

The picket used for adiabat shaping reduces laser imprint. Planar RTI x-ray radiography experiments were performed with a surrogate foam target overcoated with a thin layer of plastic (see figure 3(*a*)) to investigate the effect of the picket pulse on laser imprint [50]. The foils were driven by a low adiabat pulse shape either without the picket or with the picket (figure 3(*b*)). The measured radiographs show significant imprint reduction with picket pulses (figure 3(*c*)). Figure 3(*d*) shows that the optical-depth modulations are significantly reduced at shorter wavelengths by using a picket pulse.

3. Symmetric-illumination direct-drive ignition

Ignition target designs are being validated with implosions on OMEGA. Cryogenic and plastic/foam (surrogate-cryogenic) targets that are hydrodynamically scaled from ignition target designs (laser energy $\sim$ target radius^3, laser power $\sim$ target radius^2 and time $\sim$ target radius) are imploded to investigate the key target physics issues of energy coupling, hydrodynamic instabilities and implosion symmetry [6, 21, 51, 52]. The all-DT, $\alpha = 3$, direct-drive ICF ignition target design for the NIF and the OMEGA $\alpha = 4$, cryogenic deuterium layered target design are shown in figure 4, along with the required laser pulse shapes. Preheat of the fuel by fast electrons generated by the two-plasmon-decay instability and radiation from the corona can adversely affect target performance. Measurements of preheat owing to fast electrons in laser implosions show that about 0.3% of incident laser energy is deposited within acceptable limits for direct-drive ICF [53].

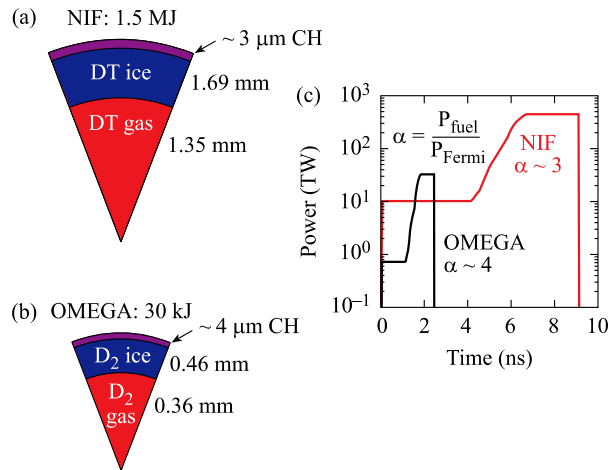Routine cryogenic target implosions on OMEGA have required significant engineering and development [54].

Figure 4. Schematic of (*a*) the all-DT, $\alpha = 3$, direct-drive ICF ignition target design developed at LLE for the NIF and (*b*) the OMEGA $\alpha = 4$, cryogenic deuterium layered target design, along with (*c*) the laser pulse shapes.

Cryogenic implosions have been carried out on OMEGA for the last three years. Significant obstacles have been overcome, including cryogenic target transport, target survival, target-layer survival and target vibration at shot time. Recently, eight cryogenic targets were shot in a single week. In a cryogenic target, perturbations of the inner ice surface seed the RTI both by feedout during the acceleration phase and by directly seeding the deceleration phase. Extensive research and development has produced ice-layer roughnesses [52, 55] approaching the 1 μm rms requirement for ignition targets. The inner-ice-surface roughness is characterized using optical
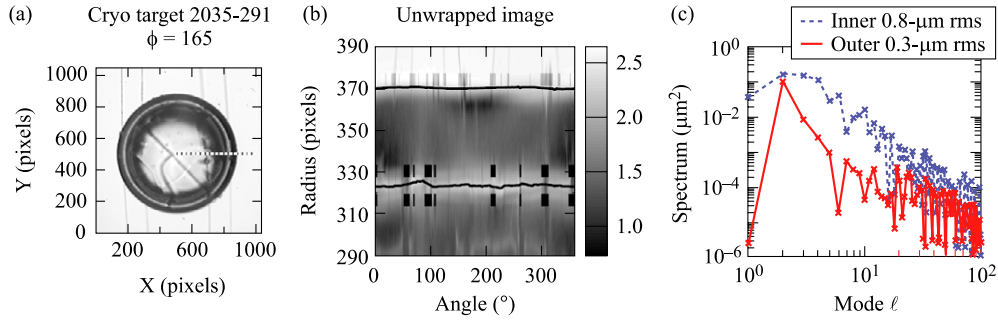
Figure 5. The inner-ice-surface roughness is characterized using shadowgraphy. (*a*) A shadowgraph of a cryogenic layer target. (*b*) The unwrapped image of the shadowgraph shows the radial location of the bright band that is used to evaluate the mode spectrum of the inner-ice-surface roughness. (*c*) Mode spectra of inner-ice-surface roughness (dotted curve (blue)) and the outer target roughness (full curve (red)).

shadowgraphy [51, 52, 55]. A shadowgraph of a cryogenic layer target is shown in figure 5(*a*). The experimental signature of the inner-ice-surface roughness is the radial location of the bright band that can be observed in the unwrapped image of figure 5(*b*). The mode spectrum of the inner-ice-surface roughness shown in figure 5(*c*) is calculated from this feature. The roughness spectrum of the outside of the CH shell is also shown in figure 5(*c*). The smoothest layers with ~1 μm rms roughness were observed in some rotational views of the target driving a requirement to measure the three-dimensional characteristics of the ice layer non-uniformity. A three-dimensional reconstruction of the inner ice layer is constructed from many views of the target, and low-order ℓ and m modes of the inner ice surface are calculated [55]. Structures in the ice correlate with known asymmetries in the layering spheres and are consistent over repeated layering/melting cycles.

The effects of laser irradiation non-uniformities and target-surface roughness on implosion performance are modelled with the two-dimensional hydrodynamic codes *ORCHID* or *DRACO* [10]. The sources for non-uniformity are (1) laser imprint associated with two-colour cycle × 1 THz 2D SSD, (2) on-target power imbalance, (3) inner-surface roughness of the ice layer and (4) outer-surface roughness of the capsule. At the end of the acceleration phase the predicted distortions on the inner ice surface can be quantified with the parameter $\bar{\sigma}$ [5], a weighted sum of the inner-ice-surface amplitude spectrum,

$$\bar{\sigma} = \sqrt{0.06 \times \bar{\sigma}_\ell^2 (\ell < 10) + \bar{\sigma}_\ell^2 (\ell \geqslant 10)}.$$

These perturbations seed the deceleration-phase RTI. A scaling of gain versus $\bar{\sigma}$ was established using two-dimensional *ORCHID* burn calculations [5]. The predicted performance of the all-DT, $\alpha = 3$ NIF direct-drive target design and the $\alpha = 4$ OMEGA cryogenic implosion predicted with $\bar{\sigma}$ is presented in figure 6. The vertical lines in figure 6 are the calculated values of $\bar{\sigma}$ on OMEGA ((red) grey dashed line) and on the NIF (black dashed line) for the NIF requirements of laser irradiation conditions of 1 THz, 2D SSD with PS and 2% rms power imbalance, and target quality of 1 μm rms inner-ice-surface roughness and 840 Å outer-surface roughness. These are predicted to lead to a normalized yield YOC of ~0.4 for the $\alpha = 4$ implosion on OMEGA. Demonstrating the $\bar{\sigma}$ scaling with yield will validate the numerical modelling of current OMEGA experiments and give confidence in the ability to
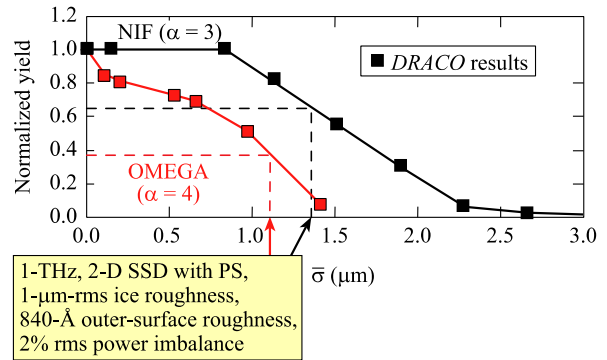

Figure 6. The performance of the all-DT, $\alpha = 3$ NIF direct-drive target design and the $\alpha = 4$ OMEGA cryogenic implosion predicted using the $\bar{\sigma}$ scaling. The vertical lines are the expected values of $\bar{\sigma}$ on the NIF (black dashed line) and OMEGA ((red) grey dashed line) with the NIF requirements for laser irradiation conditions of 1 THz, two-dimensional SSD with PS and 2% rms power imbalance and target quality of 1 μm rms inner-ice-surface roughness and 840 Å outer-surface roughness.
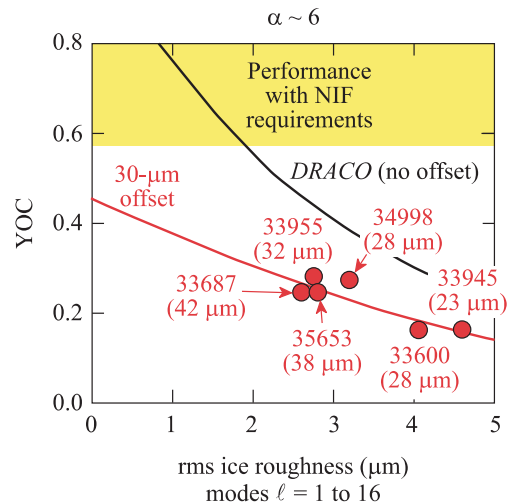

Figure 7. A comparison of the two-dimensional predicted YOC with the experimentally determined YOC for $\alpha \sim 6$ cryogenic implosions. The two-dimensional simulation with the 30 μm offset ((red) grey line) shows agreement with the experimental data ((red) grey circles). The measured target offsets for each shot are listed in parentheses. The two-dimensional simulations include the effects of the ice roughness and the laser irradiation non-uniformity owing to the target offset. The (yellow) shaded region indicates the target performance predicted with the NIF requirements.
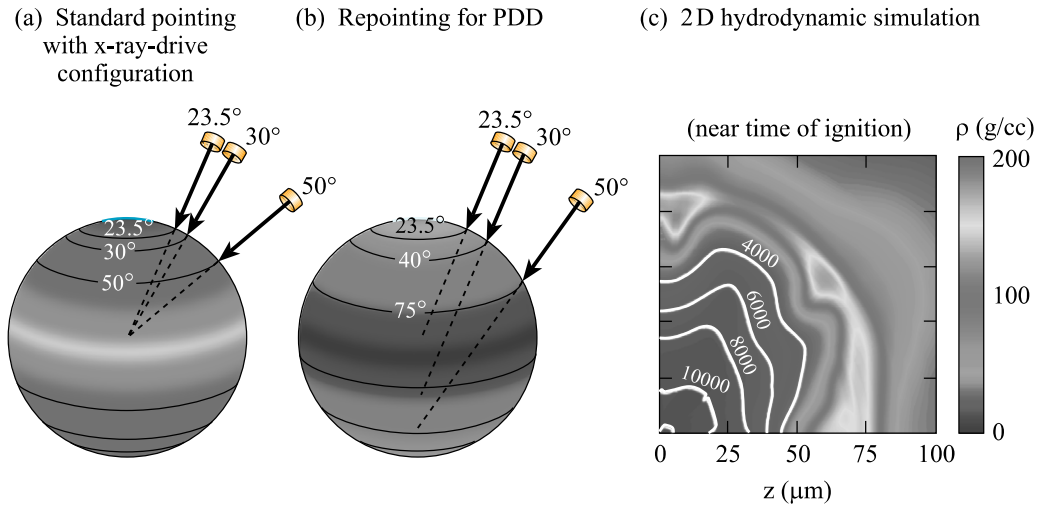
(a) Standard pointing
with x-ray-drive
configuration

(b) Repointing for PDD

(c) 2D hydrodynamic simulation

Figure 8. (*a*) The standard pointing with x-ray-drive configuration, (*b*) the repointing for PDD and (*c*) contour plots of the mass density (colour mapping) and ion temperatures (white lines) near the time of ignition from a two-dimensional hydrodynamic simulation. Initial two-dimensional simulations of the PDD target design have achieved ignition with modest gain.

predict ignition for direct-drive target designs. Applying the NIF requirements in the two-dimensional simulation of the all-DT, $\alpha = 3$ NIF direct-drive target design gives a two-dimensional predicted gain of $\sim$30 [5, 6]. Adiabat shaping boosts the stability of this design and increases the two-dimensional predicted gain to 35 [6].

The performance of imploded cryogenic D_2 capsules on OMEGA is close to the prediction of the two-dimensional hydrodynamic code *DRACO* [6, 9]. Figure 7 shows that the two-dimensional predicted YOC with a 30 μm offset is in good agreement with the experimentally determined YOC over a wide range of ice-roughness conditions for $\alpha \sim 6$ implosions. The target positioning offsets are primarily due to vibration of the spider-silk-supported targets. Uniform laser irradiation of the target is achieved when it is located at target chamber centre; hence, offsets cause low-ℓ-mode irradiation non-uniformities. These vibrations will be reduced to negligible levels with a new, more robust mechanical support. The highest average measured $\rho R \sim 100$ mg cm^{-2} is $\sim$60% of one-dimensional predictions and very close to two-dimensional predictions [9]. The current results are within a factor of $\sim$2 of achieving the NIF requirements on OMEGA. The hot-spot n_e and T_e profiles of an imploded cryogenic D_2 target inferred with gated x-ray core images and secondary neutron measurements are close to one-dimensional predictions [9, 56]. The inferred isobaric core pressure is $\sim$5 Gbar.

The path to ignition involves DT cryogenic implosions. To this end the D_2 fill and transfer station (FTS) is presently being upgraded to provide concurrent DT and D_2 cryogenic operations on OMEGA. Initial cryogenic DT implosions are expected in the summer of 2005.

4. PDD on the NIF and OMEGA

Prospects for direct-drive ignition on the NIF while it is configured in its x-ray-drive irradiation configuration are favourable with PDD [11]. The PDD approach is based on optimizing the phase plate design, beam pointing and pulse shaping to minimize the spherical drive non-uniformity
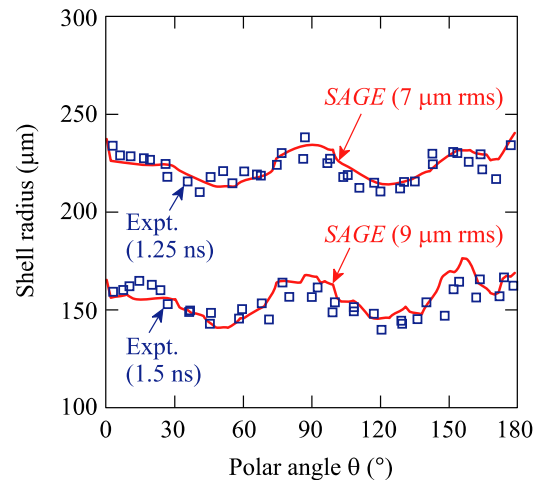

Figure 9. A comparison of the measured non-uniformities (blue symbols) in the imploding shell of a PDD target on OMEGA with the simulation (red curves) for two times during the implosion.

on an ignition capsule for the nonsymmetric illumination configuration of the NIF in its indirect-drive configuration. The baseline PDD design uses a scaled version of a NIF high-performance, wetted-foam, direct-drive target design. The equivalent one-dimensional design absorbs 95% of the 1.1 MJ incident on the target. It has an implosion velocity of 4×10^7 cm s^{-1}, a peak ρR of 1.2 g cm^{-2} and a gain of 54. Figure 8 shows the standard pointing with the x-ray-drive configuration in (*a*), the repointing for PDD in (*b*) and contour plots of the mass density and ion temperature near the time of ignition from a two-dimensional hydrodynamic simulation in (*c*). Initial two-dimensional simulations of the PDD target design predict ignition with modest gain. PDD trades high gain for increased laser irradiation non-uniformity [11].

PDD simulations are being validated in experiments on OMEGA. The NIF PDD configuration with 48 quads was approximated by repointing 40 beams of OMEGA. Experiments on OMEGA measured the non-uniformities in the imploding shell using x-ray radiography [12]. In this
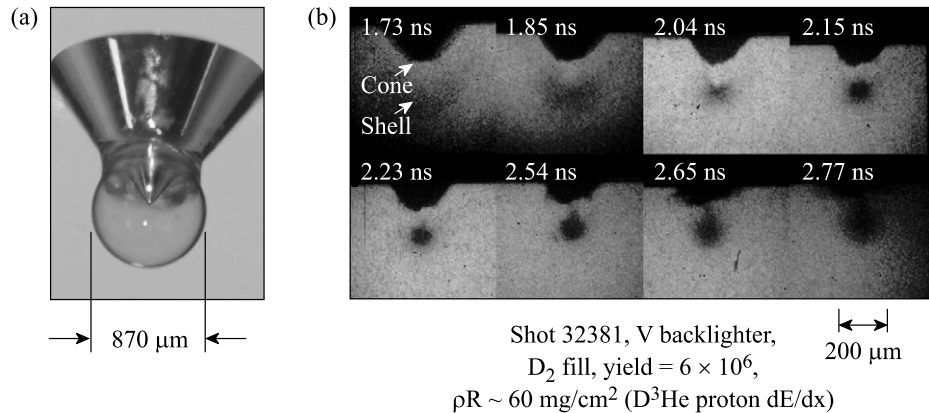
Figure 10. (*a*) A gas-tight FI target with a Au cone developed for fuel-assembly experiments was imploded on OMEGA. (*b*) A time sequence of backlit x-ray-framing-camera images shows the core assembly and cone reaction in great detail.

case, the target was a 20 μm thick CH shell filled with 15 atm of D_2 gas. Figure 9 shows the nonspherical shell radius as a function of azimuthal angle at two different times during the implosion, with *SAGE* hydrodynamic simulations agreeing with experimental observations. *SAGE* is a two-dimensional Eulerian hydrodynamics code with a self-consistent ray-trace treatment of laser absorption [57]. *DRACO* [10] simulations of x-ray emission from the PDD experiments qualitatively reproduce the shape of the compressed core.

5. FI research on OMEGA

The FI concept for ICF [13] is an active area of research at LLE. Higher gains are predicted with FI than with hot-spot ignition; consequently, ignition could be achieved with lower drive energies. A HEPW capability is being constructed at LLE next to the existing 60-beam OMEGA facility. The OMEGA EP (extended performance) laser will add two short-pulse (10 ps to ~100 ps), 2.6 kJ beams to the OMEGA laser system to study FI physics with focused intensities up to 6×10^{20} W cm^{-2}. The HEPW beams will be integrated into the OMEGA compression facility for experiments beginning in 2008. Experiments designed to validate FI will be performed with scaled cryogenic capsules. A high-density fuel configuration will be assembled with the OMEGA compression facility, and the OMEGA EP will produce suprathermal electrons via high-intensity laser–plasma interaction to heat the core.

Surrogate direct-drive, fuel assembly implosions with FI cone targets have been performed on OMEGA with a substantial fraction of the predicted core areal density measured. Gas-tight FI targets with a Au cone developed for fuel assembly experiments (see figure 10(*a*)) were imploded on OMEGA [14]. The Au cone had a 35° half-angle. The target was filled with 10 atm of D_2 or D^3He. The plastic shell had a 24 μm thick wall and an 870 μm outside diameter. As shown in figure 10(*b*) the backlit framing camera images show the core assembly and cone reaction in great detail [15]. A neutron-burn-averaged $\rho R \sim 60$ mg cm^{-2} was inferred from the energy loss of the D^3He protons [23].

6. Conclusions

The achievement of thermonuclear ignition with direct drive on the NIF, or any other MJ-class laser system, is extremely promising. Significant experimental and theoretical progress has been achieved by LLE's direct-drive ICF programme, charting the path to ignition. High-performance layered deuterium cryogenic targets are imploded on OMEGA to validate the hydrodynamic codes used to design direct-drive-ignition targets. Initial cryogenic DT implosions are expected on OMEGA in the summer of 2005. Symmetric direct drive on the NIF is predicted to achieve high gain (~35) with adiabat shaping. Prospects for direct drive on the NIF while it is in its x-ray-drive irradiation configuration are also extremely favourable with PDD. Initial two-dimensional simulations of the PDD target design have shown ignition with modest gain. Fully integrated FI experiments will begin on the OMEGA compression facility once the HEPW upgrade—OMEGA EP—is completed in 2007.

References

[1] Sethian J.D. *et al* 2003 *Nucl. Fusion* **43** 1693
[2] Schmitt A.J. *et al* 2004 *Phys. Plasmas* **11** 2716
[3] Mima K. 2004 *Nucl. Fusion* **44** S129
[4] Lindl J.D. 1998 *Inertial Confinement Fusion: The Quest for Ignition and Energy Gain Using Indirect Drive* (New York: Springer)
[5] McKenty P.W. *et al* 2001 *Phys. Plasmas* **8** 2315
[6] McKenty P.W. *et al* 2004 *Phys. Plasmas* **11** 2790
[7] Paisner J. *et al* 1994 *Laser Focus World* **30** 75
[8] Boehly T.R. *et al* 1997 *Opt. Commun.* **133** 495
[9] Marshall F.J. *et al* 2005 *Phys. Plasmas* **12** 056302
[10] Radha P.B. *et al* 2005 *Phys. Plasmas* **12** 032702
[11] Skupsky S. *et al* 2004 *Phys. Plasmas* **11** 2763
[12] Craxton R.S. *et al* 2005 *Phys. Plasmas* **12** 056304
[13] Tabak M. *et al* 1994 *Phys. Plasmas* **1** 1626
[14] Stoeckl C. *et al* Fuel assembly experiments with gas-filled, cone-in-shell, fast-ignitor targets on OMEGA *Phys. Rev. Lett.* submitted
[15] Stephens R.B. *et al* 2005 *Phys. Plasmas* **12** 056312

[16] Bodner S.E. *et al* 1998 *Phys. Plasmas* **5** 1901
[17] Regan S.P. *et al* 2004 *Phys. Rev. Lett.* **92** 185002
[18] Regan S.P. *et al Phys. Rev. Lett.* **89** 085003
[19] Bell G.I. 1951 *Report* LA-1321, Los Alamos National Laboratory, Los Alamos, NM
[20] Plesset M.S. 1954 *J. Appl. Phys.* **25** 96
[21] Meyerhofer D.D. *et al* 2001 *Phys. Plasmas* **8** 2251
[22] Li C.K. *et al* 2002 *Phys. Rev. Lett.* **89** 165002
[23] Séguin F.H. *et al* 2003 *Rev. Sci. Instrum.* **74** 975
[24] Regan S.P. *et al* 2002 *Phys. Plasmas* **9** 1357
[25] Smalyuk V.A. *et al* 2001 *Phys. Rev. Lett.* **87** 155002
[26] Skupsky S. and Craxton R.S. 1999 *Phys. Plasmas* **6** 2157
[27] Skupsky S. *et al* 1989 *J. Appl. Phys.* **66** 3456
[28] Rothenberg J.E. 1997 *J. Opt. Soc. Am.* B **14** 1664
[29] Regan S.P. *et al* 2000 *J. Opt. Soc. Am.* B **17** 1483
[30] Kessler T.J. *et al* 1993 *Laser Coherence Control: Technology and Applications* (SPIE vol 1870) ed H.T. Powell and T.J. Kessler (Bellingham, WA: SPIE) p 95
[31] Lin Y., Kessler T.J. and Lawrence G.N. 1996 *Opt. Lett.* **21** 1703
[32] Kato Y. 1984 unpublished notes from work at LLE
[33] Tsubakimoto K. *et al* 1992 *Opt. Commun.* **91** 9
[34] Tsubakimoto K. *et al* 1993 *Opt. Commun.* **103** 185
[35] 1990 *Laboratory for Laser Energetics LLE Review* **45** 1, NTIS document No DOE/DP40200-149
[36] Gunderman T.E. *et al* 1990 *Conf. on Lasers and Electro-Optics* (Washington, DC: Optical Society of America) p 354
[37] Boehly T.R. *et al* 1999 *J. Appl. Phys.* **85** 3444
[38] Marshall F.J. *et al* 2004 *Phys. Plasmas* **11** 251
[39] 2004 *Laboratory for Laser Energetics LLE Review* **98** 49, NTIS document No DOE/SF/19460-527
[40] Lehmberg R.H. and Obenschain S.P. 1983 *Opt. Commun.* **46** 27
[41] Regan S.P. *et al* 2004 *Bull. Am. Phys. Soc.* **49** 62
[42] Betti R. *et al.* 1998 *Phys. Plasmas* **5** 1446
[43] Herrmann M.C., Tabak M. and Lindl J.D. 2001 *Phys. Plasmas* **8** 2296
[44] Betti R. *et al* 2002 *Phys. Plasmas* **9** 2277
[45] Goncharov V.N. *et al* 2003 *Phys. Plasmas* **10** 1906
[46] Anderson K. and Betti R. 2004 *Phys. Plasmas* **11** 5
[47] Anderson K. and Betti R. 2003 *Phys. Plasmas* **10** 4448
[48] Lindl J.D. and Mead W.C. 1975 *Phys. Rev. Lett.* **34** 1273
[49] Metzler N. *et al* 2002 *Phys. Plasmas* **9** 5050
[50] Knauer J.P. 2005 *et al Phys. Plasmas* **12** 056306
[51] Stoeckl C. *et al* 2002 *Phys. Plasmas* **9** 2195
[52] Sangster T.C. *et al* 2003 *Phys. Plasmas* **10** 1937
[53] Yaakobi B. *et al* 2000 *Phys. Plasmas* **7** 3714
[54] 2004 *Laboratory for Laser Energetics LLE Review* **99** 160, NTIS document No DOE/SF/19460-555
[55] Meyerhofer D.D. *et al* 2003 *Bull. Am. Phys. Soc.* **48** 55
[56] Smalyuk V.A. *et al* 2005 *Phys. Plasmas* **12** 052706
[57] Craxton R.S. and McCrory R.L. 1984 *J. Appl. Phys.* **56** 108